Numerical prediction of non-linear rheology of branched polymer melts

Chinmay Das,[1, a)] Daniel J. Read,[2, b)] Dietmar Auhl,[3, c)] Michael Kapnistos,[4, d)] Jaap den Doelder,[5, e)] Iakovos Vittorias,[6, f)] and Tom C.B. McLeish[7, g)]

[1)]*School of Physics and Astronomy, University of Leeds, Leeds, LS2 9JT, UK*

[2)]*Department of Applied Mathematics, University of Leeds, Leeds, LS2 9JT, UK*

[3)]*Faculty of Humanities and Sciences, Maastricht University, P.O. Box 616, 6200 MD Maastricht, Netherlands*

[4)]*Plastika Kritis S.A., P.O.Box 1093, GR 711 10 Iraklion, Crete, Greece*

[5)]*Dow Benelux B.V., Performance Plastics Materials Science, P.O. Box 48, 4530 AA, Terneuzen, Netherlands*

[6)]*Bassel Polyolefine GmbH, LyondellBasell, R&D Polymer Physics and Characterization, Industriepark Hoechst, D-65926 Frankfurt am Main, Germany*

[7)]*Departments of Physics and Chemistry, Durham University, Durham DH1 3LE, UK*

(Dated: 14 March 2014)

In a recent short communication (Read *et al.*, Science, **333**, 1871, 2011), we showed that a computational scheme can describe the non-linear flow properties for a series of industrial low-density polyethylene (LDPE) resins starting from the molecular architecture. The molecular architecture itself is determined by fitting parameters of a reaction kinetics model to average structural information obtained from gel-permeation chromatography and light scattering. Flow responses of these molecules in transient uniaxial extension and shear are calculated by mapping the stretch and orientation dynamics of the segments within the molecules to effective pom-pom modes. In this paper, we provide the details of the computational scheme and present additional results on a LDPE and a high-density polyethylene (HDPE) resin to illustrate the dependence of segmental maximum stretch variables on the flow rate.

[a)]Electronic mail: c.das@leeds.ac.uk

[b)]Electronic mail: d.j.read@leeds.ac.uk

[c)]Electronic mail: dietmar.auhl@maastrichtuniversity.nl

[d)]Electronic mail: m.kapnistos@gmail.com

[e)]Electronic mail: cfdendoelder@dow.com

[f)]Electronic mail: iakovos.vittorias@lyondellbasell.com

[g)]Electronic mail: t.c.b.mcleish@durham.ac.uk

I. INTRODUCTION

Predicting the flow properties of entangled branched polymer melts from their molecular structure remains one of the hard problems of polymer physics. It also attracts, understandably, considerable industrial interest. The very large separation of the relevant relaxation timescales renders traditional molecular simulations like molecular dynamics or Monte Carlo of little use for industrial polymer resins. Similarly, extensions of liquid state theories to predict the flow properties have had limited success. However, in the last decade, considerable success has been found in the case of linear rheology by using the phenomenological relaxation mechanisms of extended tube theory (Doi and Edwards, 1986; de Gennes, 1971) to follow numerically the relaxation of a set of representative molecules defined at the segment level (Larson, 2001; Park *et al.*, 2005; Das *et al.*, 2006a). These 'hierarchical' relaxation algorithms work by using a faithful representation of the reaction chemistry to generate an *ensemble of molecules in-silico.* To probe at the experimentally relevant timescale, a description of the molecules at the level of entanglement segments suffices. After a small step strain, coupled phenomenological rules give the time relaxation of stress carrying segments at discrete times. The visco-elastic moduli are then calculated by assigning the weights calculated during the previous step to the set of Maxwell modes defined at those quasi-continuous times. This approach has met with considerable success for a wide variety of both model and industrial resins, despite requiring only two chief fitting parameters for each polymer chemistry (the chemistry-dependent entanglement molar mass M_e and the entanglement time τ_e). In addition, two more chemistry-independent, dimensionless, order-one parameters, related to the dynamic tube dilation through constraint release and the branch-point hop size, are required.

In this paper, we describe an extension of such a computational scheme for predicting the non-linear flow properties of generic branched polymer melt. The linear rheology is calculated from a set of Maxwell modes, with the weights and relaxation times of the Maxwell modes computed from following the relaxation of the representative molecules in time. Correspondingly, we calculate the non-linear rheological response from a set of pom-pom modes (McLeish and Larson, 1998), with the appropriate parameters of these pom-pom modes computed from the relaxation after a small step strain. We highlight here the four non-trivial aspects of this work at the very outset: Firstly, multimode pom-pom equations (Inkson *et al.*, 1999) frequently have been used to fit the nonlinear rheological response of branched polymers - but we are aiming for *a priori* prediction and not a fit of experimental data in this work. Thus, the priority variables and the relaxation times appearing in the pom-pom equations are endowed with a physical meaning from the topological structure and stress relaxation time-scales. Secondly, to predict the linear rheology correctly, one uses two sets of Maxwell modes - one for the stress relaxed by the chains and another for the stress carried by the tube constraints themselves. We extend the use of pom-pom modes in a manner that is consistent with this constraint release picture. Thirdly, the geometric concept of *priority variable* (Bick and McLeish, 1996) has been used in the literature to assign the maximum stretch of segments in a branched molecule. But, as we show in this work, one needs to modify the "bare" geometric priority so that it becomes flow rate dependent. Finally, it is non-trivial that the topological connectivity of the molecules and the computation required to predict the linear rheological response alone contain enough information for accurate prediction of the stress growth and relaxation in the non-linear regime. Since we know that the pom-pom equations are versatile enough to fit both the extensional

and shear results found in experiments of complex-architecture melts (McLeish and Larson, 1998; Inkson et al., 1999; Lee et al., 2001), if we find a way to assign proper weights to possibly a large number of such modes, the hope is that we can capture the non-linear rheology properly. But, the ultimate success of the scheme rests through comparison with experimental results. By comparing our predictions with the experimental data on the stress profile during startup uniaxial extension and shear flow for some industrial resins, we show that the scheme is fairly successful, given there are no extra free parameters beyond those already present for predicting the linear rheology.

The rest of the paper is organised as follows: We begin with a short recapitulation of the scheme used for predicting the linear rheology of generic branch-on-branch polymer melt (Das et al., 2006a) in sec. II. Next we give a brief summary of the pom-pom constitutive equations and previous attempts in assigning pom-pom parameters to branched polymer resins (sec. III). These two introductory sections are brief and serve only to introduce the variables used in rest of the paper. The new physics included in marrying the pom-pom equations with the hierarchical relaxation scheme is in sec. IV. Sec. V gives a detailed description of the algorithm. The scheme is included in the publicly available software to calculate rheological properties (Das, 2012). We consider an industrial branched low-density polyethylene resin (LDPE) and a metallocene catalysed high-density polyethylene (HDPE) resin to test the predictive power of the algorithm in VI.

A short description of the algorithm and results on a series of LDPE resins have been published elsewhere (Read et al., 2011). The description of the algorithm in that work was necessarily too short to provide all the important details for a critical evaluation of the scheme, or for others to build on this work. We end this paper with a summary including our own views of shortcomings in the scheme and an outlook on the possible extensions to this work.

II. COMPUTATIONAL LINEAR RHEOLOGY

The generalisation of the process of arm-retraction from simple entangled star polymers (Milner and McLeish, 1997) to more complex branched architecture was initially investigated analytically in a few simple cases (McLeish, 1988; Rubinstein et al., 1990). The coupled nature of the relaxation prohibits an analytical description without drastic simplifications for industrially relevant resins with large topological polydispersity. Larson (2001) introduced the 'hierarchical' numerical relaxation scheme based on the tube model of de Gennes (1971) and Doi and Edwards (1986) for branched polymer melts. Das et al. (2006a) extended the scheme for generic branch-on-branch polymers. For distinguishing between the two, we use the already common terminology of 'hierarchical model' for (Larson, 2001, and extensions by Larson and collaborators) and 'BoB' for (Das et al., 2006a). For molecules which can be cast as a comb or star polymer, both models follow very similar physics and differ only in details. A comparative analysis of the two has been recently done by Wang et al. (2010). We should also note here a rather different approach for numerical prediction of linear rheology by van Ruymbeke et al. (2006). Of these, only the 'BoB' code is generic enough to handle the highly branched structure that arises in polymers like LDPE.

A number of articles already cover the methodology used in calculating the rheological response of branched polymers in the linear regime in BoB (Das et al., 2006a,b; Wang et al., 2010). We only summarise the main ideas here, chiefly to introduce the variables that are required in the calculation of the non-linear rheology.
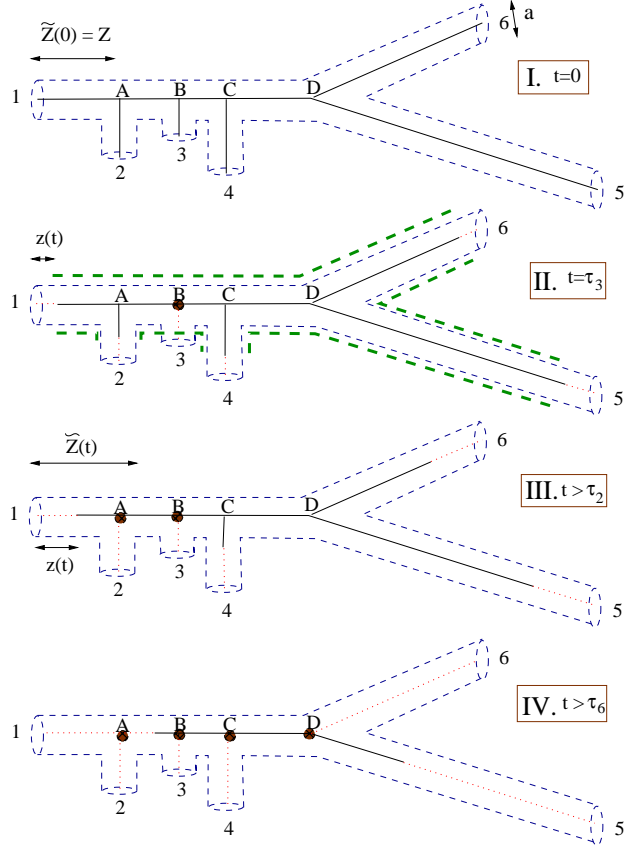
FIG. 1. Schematic representation of hierarchical stress relaxation: (I) Relaxation of stress carried by a given polymer (represented by solid line) after a small step strain is hindered by the tube potential (diameter a, drawn as dashed line). Free-ends (labelled by numbers) of length Z retract as star-arms. (II) For $t > \tau_3$ (the retraction time of segment 3) the branch-point B provides localised friction (indicated by filled circle). The relaxation of material softens the confining potential, indicated by thick dashed lines around the original tube. $z(t)$ designates the length of the original tube segment lost at time t, measured from the end-monomer of a free-end. (III) Beyond τ_2, the relaxation time of segment 2, the free-end 1 can retract by any combination of the inner segments, hindered by the localised frictions from the relaxed side-arms. This assigns a dynamics to $\tilde{Z}$, the pivot point of retraction, determined by the localised frictions at branch-points. (IV) At long times (here, $t > \tau_6$), the unrelaxed segments behave like a linear molecule and can relax by reptation.

Fig. 1 summarises the relaxation schemes considered in computational linear rheology. In the dense environment of melt, the topological constraint of non-crossing gives rise to the effective confinement of a given strand of a molecule in a tube potential due to all the other molecules. The tube diameter a sets the length scale for the problem. The entanglement molar mass M_e, the molar mass of a chain having the same size as the tube diameter, is used to express the length Z of the polymer segments. The entanglement time τ_e, the Rouse relaxation time for a linear polymer of length equal to the tube diameter, is used as the unit of time.

After a small step strain, at early times, only the chain ends can explore new conformations through withdrawal in the tube and subsequent sampling of uncorrelated tube constraints. In this process, the stress carried by the part of the old tube, that is renewed,

is lost. The variable $z(t)$ defines the length of the tube, measured from the free end, that has relaxed. Once, a *side arm* retracts its whole length (at time τ_a), it assigns an extra drag ζ_a on the *backbone*, localised at the branch point, given by

$$\zeta_a = \frac{2k_B T \tau_a}{p^2 a(\tau_a)^2},\tag{1}$$

where k_B is the Boltzmann constant and T is the temperature. The parameter p fixes the diffusive hop length scale and $a(\tau_a)$ is the tube diameter relevant at τ_a. Strands with one or more localised drag-points from side-arm collapse are termed *compound arms*. The arm-retraction mechanism becomes more subtle when branch-points on compound arms, deeper than the currently-relaxing tube segments, become mobilised themselves. The subsequent fluctuations of such branch points can contribute to the relaxation of the free ends. A good approximation to this retraction of compound arms considers an effective segment length $\tilde{Z}$, which itself has a Rouse-like dynamics with friction centres coming from the relaxed side-arms (Das *et al.*, 2006a). $\tilde{Z}(t)$ gives the pivot point about which the compound arm undergoes coherent fluctuations at time t. Equivalently, the time t at which $\tilde{Z}$ reaches a certain part of a molecule assigns an approximate Rouse time for that part. Once the leftover backbone becomes effectively linear, it can relax by reptation - a faster mechanism compared to deep arm-retraction.

Since the tube constraint is due to all the other molecules, which themselves are relaxing at the same time, the tube constraint is itself time dependent. Phenomenologically (with some scaling level theoretical backing (Colby and Rubinstein, 1990)), this is described by tube dilation - where the tube diameter scales with ϕ, the amount of unrelaxed material $(a(t) = a\phi^{-\alpha})$. Thus, with relaxation, the tube diameter increases (the confining potential softens), which in turn increases the rate of relaxation. The coupling between the different molecules is expressed by determining the tube diameter in a self-consistent way. The current effective/dilated tube at relaxation time t is termed the "supertube". The entanglement density experienced by the segments due to the supertube is denoted by $\phi_{ST}(t)$. Except for those times in which some fraction of the molecules undergoes rapid relaxation, ϕ_{ST} follows ϕ.

Fig. 1 illustrates the above relaxation mechanisms for a specific molecule. In particular, it shows: (I) the initial unrelaxed topology of the molecule in tube co-ordinates; (II) relaxation of side arms, with corresponding tube dilution and softening of the potential; (III) full relaxation of side arms and mobilisation of branchpoints, allowing deeper relaxation of a compound arm; (IV) terminal relaxation by reptation of a linear-like segment. A detailed commentary of these stages for the specific molecule is given in the figure caption.

The stress relaxation is calculated as

$$G(t) = G_0 \int_0^\infty e^{-t/\tau} \left[-\frac{d}{dt} \left(\phi(t)\phi_{ST}(t)^\alpha \right) \right]_\tau d\tau.\tag{2}$$

Here, G_0 is the plateau modulus ($G_0 \simeq \frac{4}{5}\frac{cRT}{M_e}$, with c being the polymer density and R the universal gas constant).

III. PRIORITY VARIABLE AND POM-POM CONSTITUTIVE EQUATIONS

Bick and McLeish (1996) introduced the concept of priority variable to describe the
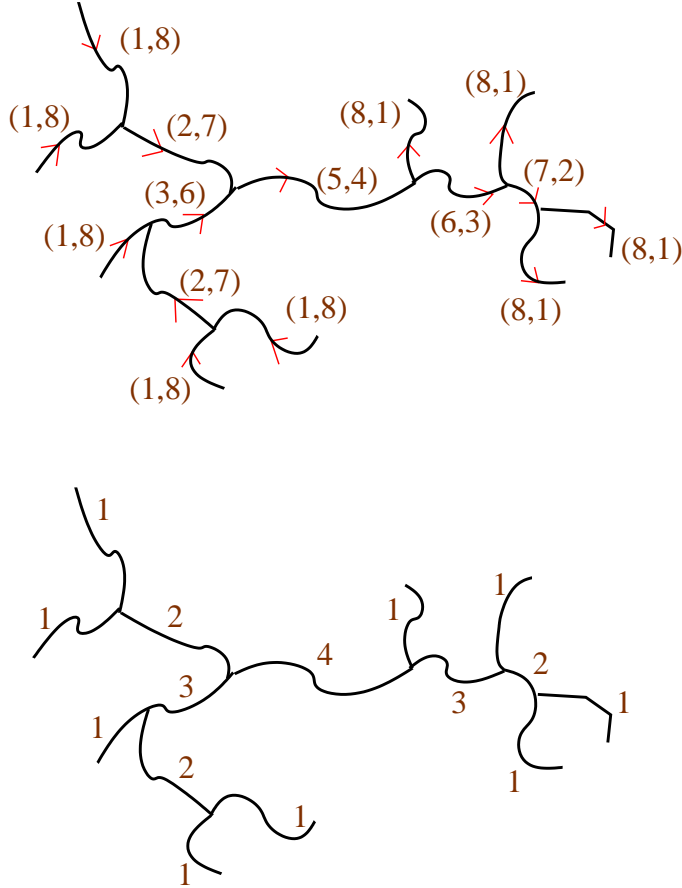
FIG. 2. Priority variables for a branched molecule. (a) For a given strand, we count n_L, the number of free ends on the left (against the arrow), and n_R on the right (along the arrow heads). (b) Geometric priorities are defined by the smaller of these two numbers.

damping function for the nonlinear stress relaxation in polymers containing long-chain branching, where the experimental damping function for the relaxation modulus is found to be much weaker than that predicted by the Doi-Edwards damping function. A large strain increases the contour length between branch points, which are not (initially) free to retract along confining tubes in the same way as a free end. The consequent segmental stretch enhances the elastic stress. However, at higher strains, an imbalance in the tensions along segments connected to a branch point can cause "branch point retraction" along the tube containing the most stretched segment. At short times, the force balance at the branch points gives a maximum tension needed before the branch point can retract. For a chain segment between branch points, priority was defined as the ratio of the maximum permissible tension to the equilibrium tension of that chain segment. The entropic nature of the tensions give rise to a simple geometrical picture (Fig. 2). For any given strand, one counts the number of free end on the left n_L and the same on the right n_R of that segment. The minimum of these two defines the priority of the segment. The priority is the value of the local chain stretch at the point of branch point withdrawal; the chain segment is assumed to maintain that maximum stretch at all higher strains.

For a general long chain branched polymer, the relaxation times vary widely (relaxation time depends exponentially on the 'depth' of a segment in a molecule). Thus the geometric
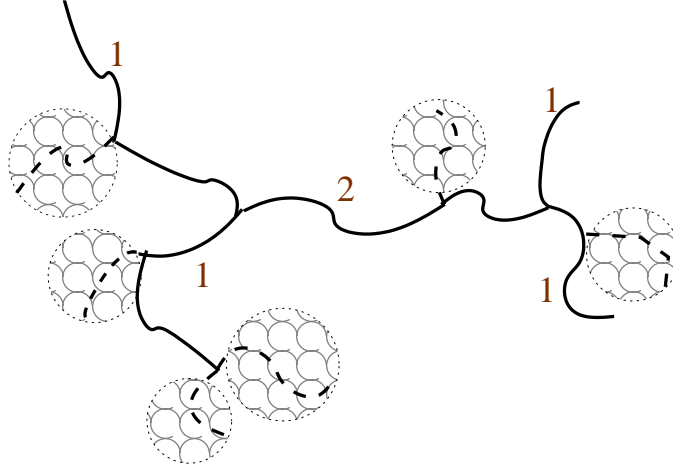
6

FIG. 3. "Snipped" priority (Read and McLeish, 2001) for the same molecule as in fig 2 at a certain flow rate. The segments having relaxation times shorter than the inverse flow rate are replaced by 'blobs' signifying localised frictional drags.

criteria given above does not capture the maximum tension in a given segment at all flow rates. Read and McLeish (2001) introduced the idea of "snipped" priority. They identified a timescale associated with the flow (τ_F, the inverse of flow-rate) and suggested that segments which relax faster than this time-scale should be neglected in calculation of the priority. Thus, in Figure 3, the segments having relaxation times shorter than τ_F are replaced by 'blobs' signifying localised frictional drags, which do not contribute to the priority calculation. Effectively the molecule in Figure 3 behaves like an 'H' polymer with a single backbone capable of supporting a (dimensionless) stretch of $\lambda = 2$. The "snipped" priority underestimates the extension hardening severely; this was clear in the original work of Read and McLeish (2001), even bearing in mind the approximations in their scheme. We confirm this observation more quantitatively below in Fig. 8. Nevertheless, the concept of a "snipped" priority gives useful insights towards building a model for flow-modified priority developed in this work.

A simpler class of polymers, pom-pom polymers comprising a single backbone with q identical side arms at the both ends, allow a simple constitutive equation that successfully capture the stress profile in nonlinear flow (Bisko *et al.*, 1997; McLeish and Larson, 1998). The number of side arms q gives the maximum permissible tension on the backbone and hence gives the priority of the backbone. The pom-pom equations are simple because all the side arms have the same timescales of retraction and the stress contribution is assumed to be dominated by the backbone. The dynamics of the stretch relaxation of the backbone is governed by the balance of the entropic tension and the localised frictional force at the branch-points. This gives an upper bound on the elastic force and hence on the stretch λ of the backbone. For faster flow, the branch-points will withdraw in the backbone tube and no further increase of stretch is possible. McLeish and Larson (1998) also considered the coupled dynamics for the branch-point withdrawal. Later authors (Inkson *et al.*, 1999; Blackwell *et al.*, 2000) neglected this dynamics of branch-points because of the large separation of timescales for branch-point withdrawal and stretch relaxation. For a numerical calculation, as in this work, the natural choice is the differential approximation of the con-

stitutive equation connecting the stress $\underline{\underline{\sigma}}$ with the orientational tensor $\underline{\underline{S}}$:

$$\underline{\underline{\sigma}} = 3G\lambda^2(t)\underline{\underline{S}}, \tag{3}$$

with $\underline{\underline{S}} \equiv \underline{\underline{A}}/\text{tr}\left(\underline{\underline{A}}\right)$ determined through the auxiliary tensor $\underline{\underline{A}}$ satisfying the upper convective Maxwell model

$$\frac{D}{Dt}\underline{\underline{A}} = \underline{\underline{K}} \cdot \underline{\underline{A}} + \underline{\underline{A}} \cdot \underline{\underline{K}}^T - \frac{1}{\tau_o}\left(\underline{\underline{A}} - \underline{\underline{I}}\right). \tag{4}$$

Here, $\frac{D}{Dt} \equiv \frac{\partial}{\partial t} + \mathbf{v}.\nabla$ is the convective derivative, $\underline{\underline{K}}$ is the deformation rate tensor, $\underline{\underline{I}}$ is the identity tensor, and τ_o is the orientational relaxation time of the backbone. The dynamics of the stretch λ is given by

$$\frac{D}{Dt}\lambda = \lambda\underline{\underline{K}} : \underline{\underline{S}}^T - \frac{1}{\tau_s}\left(\lambda - 1\right)\exp\left[\frac{2}{q-1}(\lambda - 1)\right], \tag{5}$$

with τ_s being the stretch relaxation time of the backbone. For an ensemble of different pom-pom molecules, the stress is assumed to be additive. Thus each of the pom-pom molecules are characterised by its weight fraction determining G in the stress contribution, number of side-arms at each end q, the orientational relaxation time τ_o and the stretch relaxation time τ_s. The lengths of the backbone and the dangling arms together determine the prefactor G in the stress equation in the original formulation.

IV.   COMPUTATIONAL NON-LINEAR RHEOLOGY

The simplicity of obtaining the numerical solution for non-linear flow behaviour of pom-pom model led to considerable work towards mapping an arbitrarily branched molecule to pom-pom modes. Multi-mode pom-poms have been used successfully to fit the non-linear extensional and shear rheology data (Inkson *et al.*, 1999). The distributions of the time-scales and of the priorities for highly branched resins like LDPE do not strongly depend on the number of modes selected for data fitting, which suggests that the continuous limiting form of the fitting parameters as a function of mode relaxation time may have direct relationship to the polymers themselves. However, when one considers modelling of simple polymers, where the structure is known, the fitting parameters in general do not bear any resemblance to the geometric priority q or snipped priority q_S (Inkson *et al.*, 1999). Thus, in spite of considerable success of fitting both extensional and shear startup, extension hardening and shear thinning at a number of flow rates, such exercises so far lacked predictive power for a resin where the structure is known but the rheological data is absent on which to fit the model parameters.

A.   Pom-pom modes accounting for distribution in orientational relaxation times

The resolution in pom-pom modes must reproduce the linear envelope decided by the linear rheology. Coarse-graining over a time interval Δt at t_M, eqn. 2 resolves the stress relaxation to a set of Maxwell modes with the associated modulus $g_M(t_M)$ given by

$$-\frac{g_M}{G_0} = [\phi_{ST}^\alpha]\,\Delta\phi + \left[\alpha\phi_{ST}^{\alpha-1}\phi\right]\Delta\phi_{ST}. \tag{6}$$
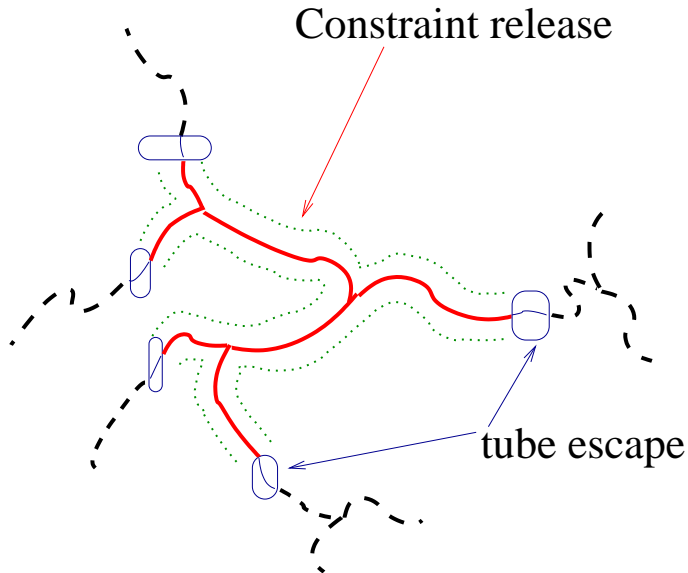
8

FIG. 4. Molecular contributions to stress decay: The boxed thin lines represent parts of the molecule having relaxation time τ_M and contributes as 'tube escape pom-pom modes'. The inner segments (represented by thick lines enclosed in dotted representation of the tube) are still to escape from the tube. These inner-segments contribute to relaxation by constraint release and decide the 'constraint release pom-pom modes'.

Here, $\Delta\phi$ is the change in the amount of unrelaxed fraction in the time interval Δt and $\Delta\phi_{ST}$ is the change in the entanglement density experienced at the same interval. We interpret the two terms on the right-hand side of eqn. 6 containing $\Delta\phi$ and $\Delta\phi_{ST}$ respectively as describing the stress relaxation due to escape from the confining tube constraint and due to the constraint release on the remaining chains trapped in the tube potential at this time scale (Fig. 4). This prompts us to consider two separate sets of pom-pom modes: 'tube escape modes' and 'constraint release modes'. Both of these two sets of modes share the same orientational relaxation time ($\tau_o = \tau_M$) but the priority and the stretch relaxation time distribution are determined by the currently relaxing parts of the chains for the tube escape modes, and by the unrelaxed part of the chains for the constraint release modes.

B. Stretch time distribution

Stretch in a part of a molecule relaxes via motion in which chain tension acts against local friction: either monomeric friction from the background melt or, in the case of a compound branched arm, much larger friction arising from side chain motion. For the outer-most branches, we consider that chain tension balances monomeric friction only, so that $\tau_s = z^2\tau_e/4$ (obtained as the Rouse time of that arm, when pinned at one end). For inner-segments, we require the effective "Rouse time" when friction is considered to arise from side arms. Fortunately, the relevant calculation is already embedded within the original BoB algorithm since, as outlined in section II, the pivot point location $\tilde{Z}(t)$ is obtained as the length of chain with effective Rouse time equal to t. Thus, we can find the stretch relaxation time τ_s of a particular chain segment simply by inverting the function $\tilde{Z}(t)$, to find the time at which $\tilde{Z}(t)$ reaches that segment.

For the constraint release pom-pom modes, we assign τ_s values that are the same as their orientational relaxation times. Our rationale for this is that constraint release gives a motion of the tube contour similar to that of a simple Rouse chain (Klein, 1978; Vivoy *et al.*, 1991), which relaxes both stretch and orientation at the same rate (Doi and Edwards, 1986). The best way of approximating this within the pom-pom model is to set the stretch relaxation time equal to the orientational relaxation time.
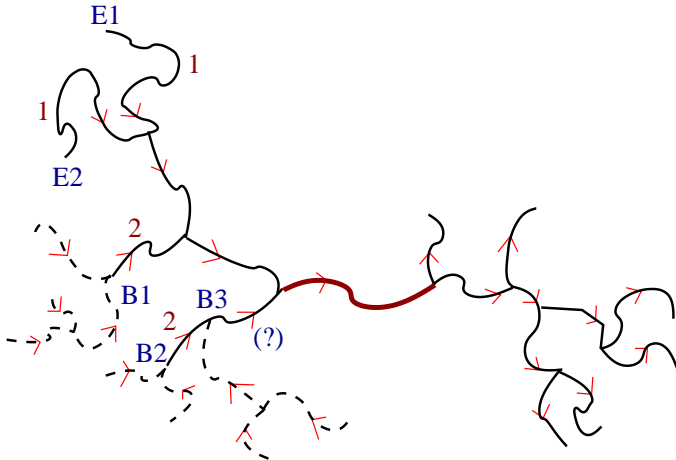
C. Flow modification of priority

FIG. 5. Assignment of flow-modified priority at flow rate $1/\tau_{\mathrm{F}}$: Segments with $\tau_s < \tau_{\mathrm{F}}$ are described by broken lines. To calculate the effective priority of the thick segment, we travel left along the molecule. At end points like $E1$ and $E2$, where end-segments have $\tau_s > \tau_{\mathrm{F}}$, the segments are assigned a value 1. At a branch-point like $B1$, where both the segments have $\tau_s < \tau_{\mathrm{F}}$, the segment before the branch-point is assigned a value 2 irrespective of level of branching outwards from the branch-point. Several possibilities need to be considered in cases where one segment at the branch point has $\tau_s < \tau_{\mathrm{F}}$ and the other has $\tau_s > \tau_{\mathrm{F}}$ (like at branch point B3). If the segment with $\tau_s < \tau_{\mathrm{F}}$ has $\tau_o > \tau_{\mathrm{F}}$, it can maintain a tension difference of 1 and gives a contribution of 1 to the priority sum. Else, we consider the equilibration time of the branch-point by calculating the Rouse time of inner segments of B3 including the friction from collapsed side-arm. B3 can maintain a tension difference and contributes to the priority sum if this equilibration time is greater than τ_{F}.

In fig. 5, we consider a generic polymer to enquire about the priority one should assign to a particular segment at a particular flow rate (with associated flow time scale τ_{F}, which is the inverse of the flow rate). Following on from the concepts of "snipped priority" introduced by Read and McLeish (2001), we recognise that at different flow rates a given segment will have different effective values for its maximum stretch, due to relaxation of other chain segments. The main innovation introduced in Read *et al.* (2011) is to recognise that the critical issue is not (as Read and McLeish (2001) thought) the orientational relaxation time. Instead, we believe it is a question of how chain stretch is transferred from outer chain segments towards the inside of the molecule, which has to do with stretch relaxation times. Segments whose stretch relaxation time is greater than the flow time, $\tau_s > \tau_{\mathrm{F}}$, are able to transfer tension from the outside of the molecule towards the inside, whilst segments with stretch

10

relaxation time less than the flow time, $\tau_s < \tau_{\mathrm{F}}$, cannot themselves stretch and so cannot transfer tension inwards, no matter how many chain ends they are attached to.

As with the "geometric priority" introduced by Bick and McLeish (1996), we start from a given segment and initially look to one side of it (e.g. the left hand side). Rather than counting chain ends, we examine the relaxation times of each segment as we look outwards, as follows. We illustrate some of these cases for a specific molecule in figure 5, giving details specific to that molecule in the figure caption.

- For an inner segment with $\tau_s > \tau_{\mathrm{F}}$, if the two outer segments have $\tau_s < \tau_{\mathrm{F}}$, the outer segments cannot stretch. But the current segment can stretch, up to a maximum stretch of 2 (at which point, withdrawal of the branchpoint will occur). So, we add 2 to the priority sum. Two examples of this are B1 and B2 in figure 5.

- If we reach a segment with $\tau_s > \tau_{\mathrm{F}}$ and both the segments outside it have $\tau_s > \tau_{\mathrm{F}}$, all segments can stretch, and we simply proceed to find out what chain structure is beyond the two outer segments.

- For a segment with $\tau_s > \tau_{\mathrm{F}}$, but where only one of the two segments beyond it has $\tau_s > \tau_{\mathrm{F}}$, only one of the subsequent segments can stretch (an example is B3 in figure 5). For the subsequent segment that stretches (B2 in the figure), we look to see what is beyond. For the segment that does not stretch (e.g. the dashed sidebranch at B3) we need to decide whether it provides sufficient friction that this branchpoint can sustain a significant difference in stretch between the two "stretching" segments. In other words, at the current flow rate, is it possible for the stretch on the inner segment (B3) to be greater than the stretch on the outer segment (B2) by one unit? To answer this, we look at the orientation relaxation time (τ_o) of the side branch.

  - If $\tau_o > \tau_{\mathrm{F}}$, then flow is fast enough to orient the side branch, so the side chain will certainly count towards the priority and we add one to the priority sum.
  - If, on the other hand, $\tau_o < \tau_{\mathrm{F}}$, more care is required: we calculate an "equilibration time" τ_{eq} for the side branch, as detailed below. If $\tau_{eq} > \tau_{\mathrm{F}}$, then the side branch can support the tension difference, and we add one to the priority sum.

To calculate τ_{eq}, we have implemented a scheme designed specifically for situations in which different side arms along a chain are expected to have greatly varying relaxation times (as is usually the case in, for example, polydisperse industrial resins). The scheme is not expected to work well, for example, in the case of regular polymer combs in which all side arms are of similar length.

We envisage a situation in which all segments outside the side branch have reached their maximum priority, and their branch-points are now withdrawn into their tubes. For such a chain configuration, withdrawn branch-points count little towards the effective friction for motion of polymer along the tube because chain motion will simply change the degree of withdrawal of the branchpoint (and so do not require branchpoint hopping from side arm relaxation). So, we anticipate only a small amount of friction from branch-points outside the considered side branch.

Looking inwards from the current side branch, we may encounter several shorter side-branches with faster orientational relaxation times. We assume these give negligible friction in the current calculation. Eventually, we will typically find a side branch with larger

orientational relaxation time than the current one, which will act as a pivot point for local chain motion to equilibrate chain stretch. We measure the length of chain between the current side branch and the first one found inwards with larger orientational relaxation time, and this gives an effective spring constant for the local equilibration of stretch due to motion of the side branch. To locally equilibrate the chain stretch, this spring pulls against the friction from the side branch, which can be obtained from its orientation relaxation time (τ_o) using eqn. 1. The ratio of the friction constant to the chain spring constant, so obtained, gives the equilibration time τ_{eq}, used in the above calculation of priority.

The priority calculation is repeated for the right-hand side of this particular segment and as with geometric priority, the lower of the two priority sums sets the priority of the segment.

V. ALGORITHMIC IMPLEMENTATION

The linear version of the computational rheology code (previous versions of BoB) already computes the two "fronts" $z(t)$, marking the relaxation of chain ends through tube escape and $\tilde{Z}(t)$, the pivot point about which the retraction is considered at time t. The latter variable defines an approximate Rouse time of a segment of an arbitrarily branched polymer molecule and influences the dynamics of $z(t)$ internally. We identify this Rouse time as the stretch relaxation time of a segment. In the current version of the code, during the relaxation after small step strain, the segments of the polymer molecules store the times at which either $z(t)$ or $\tilde{Z}(t)$ reaches the end of the segment in concern. They respectively give the orientational (τ_o) and stretch (τ_s) relaxation times of the segments. The segments also store the friction defined from the time of complete retraction (eqn. 1). The prediction of linear viscoelastic moduli already employs the form of sum of a large number of Maxwell modes (eqn. 2). They are coarse-grained to have roughly two Maxwell modes in a decade of frequency. With a given choice of Maxwell times (τ_M), the associated weights (g_M) are unique.

To predict the non-linear flow behaviour at a given flow rate, we execute the updated code twice. In the first step, the code generates or reads in the supplied polymer ensemble, and executes the algorithm to calculate linear rheology. During this process it follows time relaxation, and outputs τ_o, and τ_s for each of the segments and $\{\tau_M, g_M\}$ associated with the linear relaxation spectrum. In the second pass of the execution, the program uses the same polymer ensemble, now decorated with the relaxation time scales, and hence amenable to computation of flow modified priority variables. During the small strain relaxation in this second execution, the program maintains separate lists accounting for material relaxing through tube escape and through constraint release. For each type of stress relaxation, the lists store the fraction of the relaxation modulus associated with a given priority, subdivided into material with different stretch times (binned in log-scale, typically with 20 bins). The contents of the lists are written to a file when the time reaches the next Maxwell time τ_M, which acts as the orientational relaxation time τ_o for the current modes (For weights at τ_M, we use averages over segments relaxing between the times $\tau_M/1.1$ and $1.1 \times \tau_M$). So, at each Maxwell time, the Maxwell mode is subdivided into a (typically large) number of pom-pom modes with different priority and stretch relaxation time. Once all of the molecules have relaxed, the pom-pom modes are used to compute the transient stresses in start up shear or start up uniaxial extensional flow.

12

A. Modelling of HDPE molecules

The HDPE resin (HDB6, The Dow chemical Company) used in this work was synthesised with single-site metallocene catalyst in a continuously stirred tank reactor (CSTR) (Wood-Adams *et al.*, 2000). The ensemble of molecules in this case can be fully characterised by just two parameters: one characterising the average molar mass and the other characterising the average number of branches. Among different possibilities, we choose these two parameters as the weight averaged molar mass (M_W) and the number averaged branch per molecule (b_m). Because the resin was prepared without any co-monomer, the amount of branching is accurately known from NMR. The weight averaged molar mass is known from GPC-MALLS. The M_W and b_m can be recast as the number averaged segment length ($M_{N,S}$) between the branch-points and a branching probability (b^U, 'up-stream' branching probability). We use a simple scheme introduced in (Das *et al.*, 2006a) to generate segment-level description of molecules representing the HDPE resin. The algorithm is based on the known statistical distribution of single-site CSTR metallocene resins (Read and McLeish, 2001). Starting from the end of the molecule at which the last monomer was added, we generate a Flory distributed segment of average length $M_{N,S}$ and use the branching probability to decide if the particular segment would end at a branch-point. If it ends at a branch-point, we continue adding branches recursively.

B. Modelling of LDPE molecules

We use a Monte Carlo method to generate a statistical representation of low density polyethylene (LDPE) molecules. Tobita (2001) used such a procedure to consider the distribution of polymer structures arising from a free-radical polymerisation occurring in a batch reactor (although the basic scheme can be generalised to other reactor types). The basic steps considered are initiation (rate R_i), chain propagation (rate R_p), branching (rate constant k_b), scission (rate constant k_s), chain transfer to small molecules (rate R_f) and termination by combination (rate R_{tc}) or by disproportionation (rate R_{td}). For the batch reaction, this generates a five parameter space of

$$
\begin{aligned}
\tau &= (R_{td} + R_f)/R_p &&\text{Termination} \\
\beta &= R_{tc}/R_p &&\text{Combination} \\
C_b &= k_b/k_p &&\text{Branching} \\
C_s &= k_s/k_p &&\text{Scission} \\
x_f & &&\text{Final conversion.}
\end{aligned}
$$

For details of the Monte Carlo scheme, and for the relevant equations, we refer the reader to Tobita (2001). Repeated application of the algorithm produces a set of molecules selected on a weight-biased basis. The position and number of all branch-points, together with the molecular weight of the strands between them, are known. If sufficient number of branched polymers are generated in this way, then one can interrogate them for statistics of the overall polymer distribution (e.g. molecular weight distribution) or use the generated molecules as input into the BoB algorithm to calculate rheology. The molecules could be used as-generated, but we save computational effort in the rheology calculation by retaining only a fraction of these molecules, chosen uniformly across the range of logarithmic molecular weights generated by the algorithm. This allows us to reduce the number of molecules

used in the rheology calculation by a factor of roughly 100; the calculations below used a representative set of around 3000 molecules, but retain many large molecules in the tail of the molecular weight distribution.

We seek to use the above algorithm as a means to model the molecular architectures present in commercial LDPEs, generated in tubular reactors. In the idealised "plug flow" limit, a tubular reactor is equivalent to a batch reactor. However, real reactors are not ideal, and we found it was usually not possible to match experimental molecular weight distributions with a single batch simulation. In the absence of detailed information of reactor variables and operation, we aimed to produce a reasonable representation of LDPE-like architectures, consistent with experimental data on molecular weight distribution and branching levels (from GPC-MALLS data). Our solution was to consider a superposition of up to three batch processes, with identical reaction parameters τ, β, C_b and C_s, but different overall conversions x_f. A possible qualitative justification for this is that pure plug flow is unlikely, and different residence times are expected across the cross-section of the reactor tube, leading to different conversions. An alternative suggestion is that broadening of molecular weight distribution is induced by multiple injection points in an idealised tubular reactor.

To reduce the parameter space, we assume no scission, i.e. $C_s = 0$, since its value appeared to be consistently small when left as a free parameter. Although there are several parameters in the reaction scheme, their effects are distinctive. Increasing τ results in shorter chain strands and smaller overall molecular weight. The value of τ could be determined to reasonable accuracy by matching the low-molecular weight tail of the molecular weight distribution. Increasing β increases molecular weight and polydispersity but without greatly affecting branch density or typical molecular weight of linear strands in the molecules. In contrast, increasing C_b increases molecular weight and polydispersity but also increases branching, giving rise to smaller chain strand lengths between branch-points.

VI. RESULTS

We have measured rheological responses of six different commercial grade LDPE samples and one HDPE sample to test the computational scheme detailed here. The rheological responses of the LDPE samples are published in a short communication (Read *et al.*, 2011). Besides the HDPE resin, we select only one of the LDPE resins (LDPE2) here to illustrate the predictions under different assumptions of the modelling. Details of characterisation and rheological response measurements can be found in the supplementary online material of our earlier publication (Read *et al.*, 2011). Molar masses and radius of gyration contractions factor (g-factor) were measured with GPC-MALLS for the LDPE samples. For the HDPE resin, branching was independently measured with NMR. Shear responses were measured on a strain controlled rheometer (ARES, Rheometric scientific) using cone and plate geometry. Optional stretching device (SER, Xpansion instruments) was mounted onto the rheometer to measure the non-linear elongational flow response.

We use tube dilation exponent $\alpha = 1$ and the branch-point hop-size $p = 1/\sqrt{40}$ that provide a good description of frequency responses of a number of resins with different architectures and chemistry(Das *et al.*, 2006a,b; Chambon *et al.*, 2008; Hutchings *et al.*, 2012). For the HDPE sample, we use $M_e = 1120$ g/mol and $\tau_e = 1.1 \times 10^{-8}$ s at 155° C. The weight average molar mass $M_W = 68000$ g/mol and the average number of branches/molecule $b_m = 0.34$ uniquely determine the HDPE resin. These parameters were determined in ear-

lier work (Das *et al.*, 2006a), where the molecular weight and branching parameters were found uniquely from the GPC and NMR measurements respectively. The rheological parameters provided an excellent fit to the linear rheology of a series of HDB resins.

Presence of comonomer and short-chain branches not accounted in our scheme affect M_e and τ_e (Chen *et al.*, 2010) and we expect them to be quite different for LDPE and HDPE resins. In our data analysis, we heuristically found that $M_e = 1600$ g/mol and $\tau_e = 5.8 \times 10^{-8}$ s at $150°$ C provide a good description of the small angle oscillatory shear data for six different LDPE resins. By fitting the low-molecular weight tail of the molar mass distribution, we fix the termination rate parameter $\tau = 1.1 \times 10^{-3}$. We consider the scission rate constant $C_s = 0$. We can fit the full molar mass distribution and the g-factor with different combinations of the other parameters. We found that fits of similar quality to the molar mass distribution and the g-factor naturally gave rise to a distribution of predictions of linear rheology. This is to be expected, since relaxation times of branched molecules depend exponentially on their branching length, so rheology is more sensitive to branching levels than the g-factor. The predicted terminal viscosity, for example, could vary within approximately half a decade. While this was sufficient to rank the LDPE resins in order of terminal viscosity, an imprecise prediction of linear rheology is not a good basis for non-linear rheology prediction. So, we further constrain the fitting by comparison with the measured linear rheology. We use two sets of such parameters that give equally good fit to the molar mass distribution, the g-factor and linear rheology. One of the sets (set1) considers the combination rate constant $\beta = 1.2 \times 10^{-4}$ and branching rate constant $C_b = 5 \times 10^{-3}$. The other set (set2) considers $\beta = 1.6 \times 10^{-4}$ and $C_b = 1.8 \times 10^{-2}$. In set1, we use three different final conversions x_f: 74% of the material with $x_f = 0.62$, 13% with $x_f = 0.25$ and the rest with $x_f = 0.05$. In set2, we use two different final conversions with 80% of the resin having $x_f = 0.185$ and the rest having $x_f = 0.032$. We use set1 to compare with experimental data. In the final part of this section, we compare between the predictions of the two sets in the linear and non-linear flow.
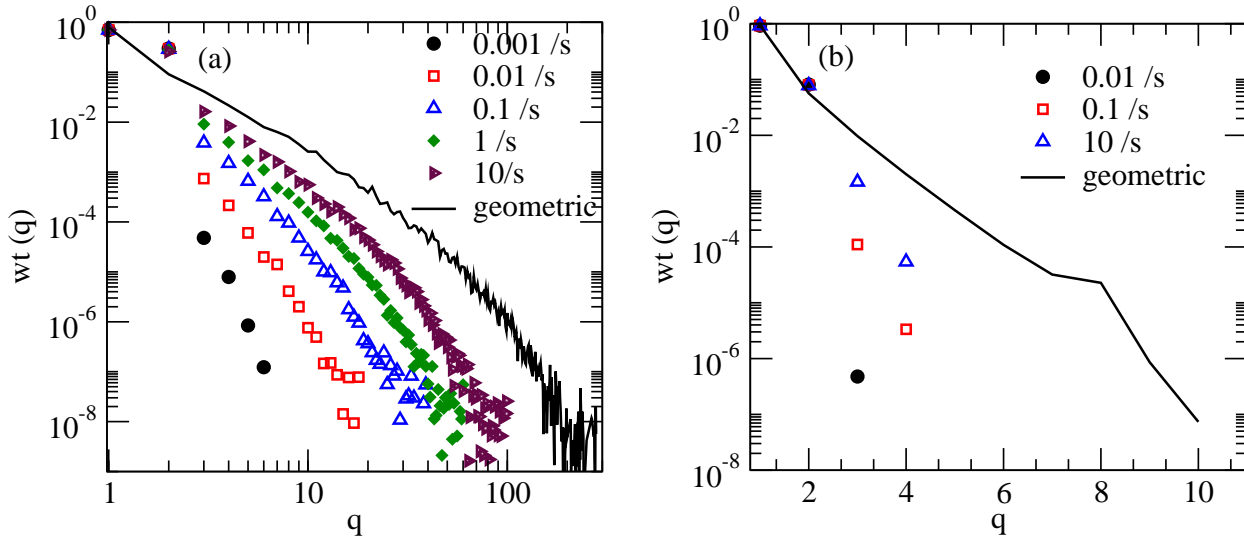

FIG. 6. Geometric (lines) and flow priorities at indicated rates (symbols) for LDPE2 (a) and HDB6 (b) resins.

The highly branched nature of LDPE2 is captured by comparing the distribution of the

priorities of LDPE2 with that of HDB6 (fig. 6). The lines in the plot indicate the weight fraction of segments with different geometric priorities. In both resins, the higher priority material accounts for a small fraction (priority one and priority two together account for 98.8% weight for HDB6 and 88.5% weight for LDPE2). For HDB6, the highest priority segment generated is 10. For LDPE2, the maximum priority is 280. We also plot flow modified priorities (symbols). As the flow rate is lowered, the effective priority of the segments change. At 0.001/s flow rate, the maximum of effective priority for LDPE2 is just 6.

From following the relaxation numerically after a small step strain, we calculate the frequency dependent visco-elastic moduli. Fig. 7 shows comparisons of our predictions with experimental data. Similar quantitative predictions are obtained using the same M_e and τ_e for a set of six LDPE (Read *et al.*, 2011) and seven HDPE samples (Das *et al.*, 2006a) having different molar masses, zero-shear viscosities and melt indices. At the lowest frequencies, our prediction for the elastic modulus is higher than the experimental data. The low frequency response is from the stress relaxation in a few highly branched molecules in our calculations. Our modelling assumes that the molecules remain entangled at all stages of relaxation. The discrepancy at low frequencies reflect breakdown of this approximation.
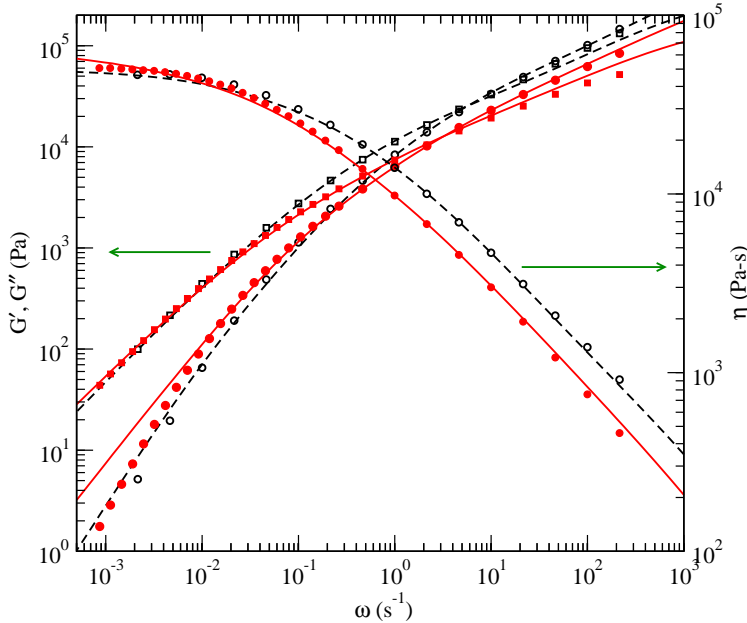

FIG. 7. Visco-elastic moduli and complex viscosity from small angle oscillatory shear experiments (symbols) and predictions (lines) for LDPE2 (filled symbols and solid lines) and HDB6 (open symbols and dashed lines).

Fig. 8 shows the start-up stress growth coefficients (transient viscosities) in extension and shear at several rates (symbols) along with predictions from our calculations (solid lines) for LDPE2 and HDB6 resins. We note here that the predictions for LDPE2 are slightly lower than Read *et al.* (2011). In the previous publication, a bug in the code erroneously assigned exactly equal weights to both the constraint release and tube escape modes. The predictions here, and the publicly released version of the code, correct that bug and follow the weight distribution assigned from Eq. 6. The corrected code consistently produces slightly lower predictions than reported in Read *et al.* (2011), with the differences for the LDPE2 resin being typical. For the LDPE2 resin, our calculations represent the linear relaxation with

55 Maxwell modes. At each of these Maxwell modes, separate pom-pom modes account for the distribution in priority and stretch time. For flow rate 0.003/s, we used in total 4587 pom-pom modes to describe the non-linear flow properties. The typical CPU time for predictions at each flow rate is of order one hour (on a single node of a Linux machine with Intel Xenon processor).

For LDPE2 resin (fig. 8a,b), we also show predictions at selected rates where we use geometric priorities (dashed lines) or fully snipped priority (dotted lines) considered in Read and McLeish (2001) to calculate the stress response. The stress response in extensional flow is highly sensitive to the assignment of priority. The geometric priority over-predicts the stress by a large amount, while the fully snipped priority significantly under-predicts the stress. With the LDPE samples containing highly branched structure, the differences in the predictions from the different schemes for assigning the priorities are dramatic. The predictions made using the stretch-based assignment of priority, as detailed in this paper, are superior to either the geometric priority or fully snipped priority predictions (a similar observation can be made for the shear predictions). They also capture well the differences in overall extension hardening behaviour between the high-density and low-density resins. Nevertheless, it is clear from figures 8(a,c) that the predictions are not perfect, and in particular there is a small underprediction of the degree of hardening at the lower extension rates. Discrepancies between our predictions and the data could be due to errors either in our values for stretch relaxation times, or in our prediction of flow-dependent priority. Since the geometric priority calculations result in consistent over-prediction, we consider it likely that the priority prediction is the likely source of remaining error. Thus, although the stretch-based assignment of priority detailed in this paper (and the approximate algorithm proposed to evaluate internal stretch equilibration times within a molecule) represents an improvement on previous suggested criteria, the scheme remains approximate and open to improvements. We discuss several possible options for this in the concluding section of the paper.

To predict the flow properties of the LDPE resin, we created the molecules by fitting the molar mass distribution and the g-factor. Fig. 9(a) shows that similar quality of fit can be obtained by quite different reaction parameters. However, despite the use of different reaction rate parameters to achieve the fit, the frequency dependent visco-elastic moduli are virtually indistinguishable for the two ensembles (fig. 9 b). The start-up stress growth coefficients in shear and extension also behave very similarly (fig. 9 c). The distributions of the priorities also are similar (fig. 9 d). This suggests that there is a degree of redundancy in the reaction model parameters: the decrease in conversion x_f in set2 as compared to set1 is largely compensated by the increase in C_b and β. There is also a degree of redundancy in the precise choice of conversions, and their respective weights, for the (up to three) superposed batch processes. Fortunately, as we show here (Fig. 9), different choices of fitting parameters that match GPC-MALLS data and linear rheology give rise to similar predictions for the non-linear rheology and have similar distributions of molecular architecture.

VII. OUTLOOK

We have described the details of a numerical scheme to compute the non-linear flow behaviour of arbitrarily branched entangled polymer melt by mapping the *in silico* molecular representation of the resin to a set of pom-pom modes. This mapping requires separate modes associated with relaxation by tube escape and constraint release. We generalise the
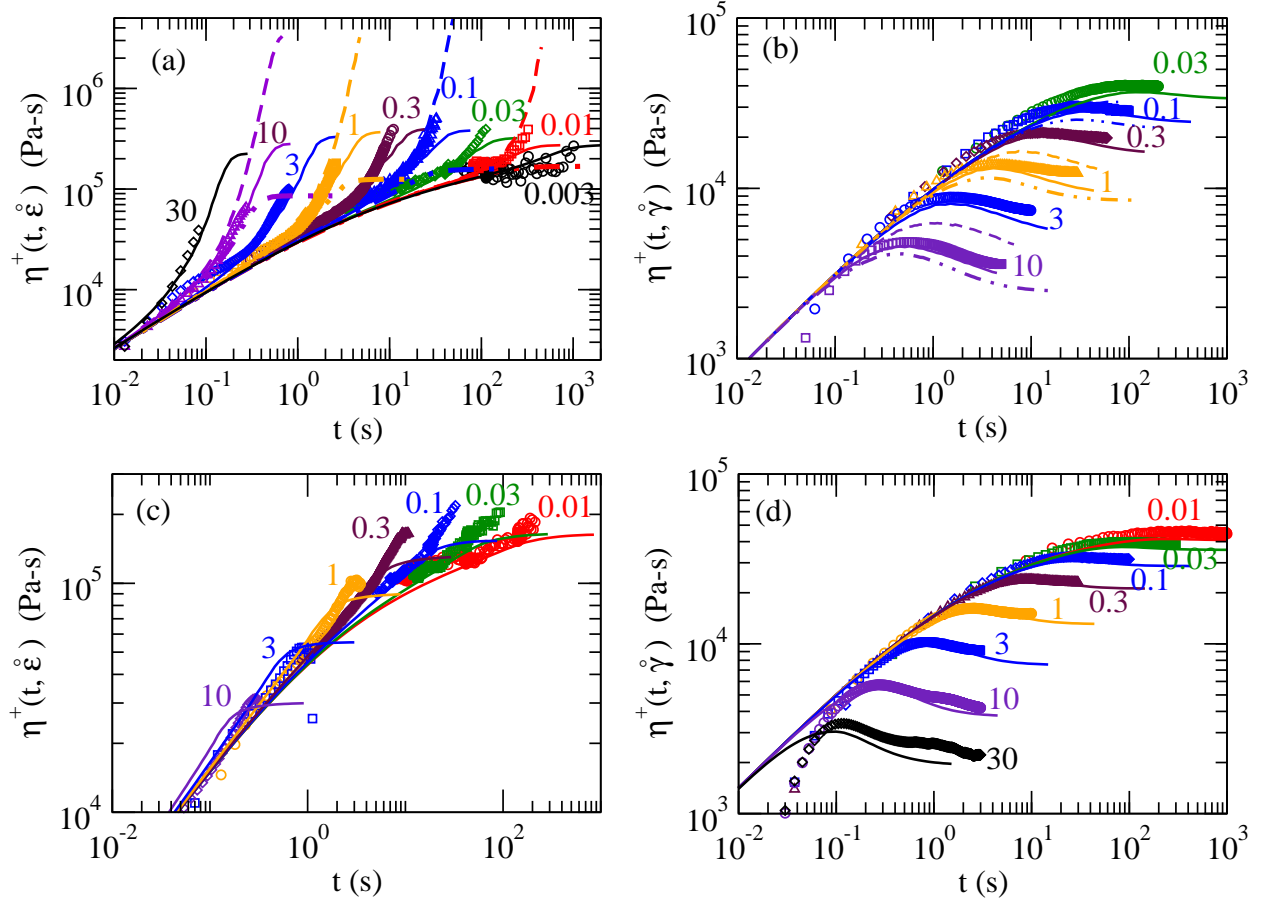
FIG. 8. Start-up stress growth coefficients in uniaxial extension (a,c) and shear (b,d) at the indicated rates in LDPE2 (a,b) and HDB6 (c,d). The experimental data are plotted as symbols. The solid lines are predictions with flow priorities. For the LDPE2 resin, we also show the predictions using geometric priority (dashed lines) and fully snipped priority (dot-dashed lines) at rates 0.01, 0.1, 1.0 and 3.0 s^{-1} for uniaxial extension (a) and at rates 0.1, 1.0 and 10.0 s^{-1} for shear (b).

topological concept of priority variables to a flow-dependent priority, which essentially counts the branch points that do not have enough time for relaxation of chain tension, i.e. it is a stretch-based criterion. This depends both on segmental stretch and orientation times and on the timescale of equilibration through coherent oscillation of segments with localised drags.

We validate our scheme by comparing with flow response of two very different commercial resins: a highly branched LDPE and a sparsely branched HDPE resin. The agreement with flow response in both the linear and the non-linear regime suggests that one can in principle use computational schemes to decide on the synthesis parameters that generate resins with desired flow properties.

The assignment of the priority variables in this work exploits the broad distribution of relaxation times in industrial resins. We use this when considering, at an approximate level, the internal dynamics of stretch propagation within a randomly branched molecule. This approximation is evident in the calculation of a local stretch equilibration time, τ_{eq}, for a given side branch in section IV(C), which exploits a hypothesised wide separation
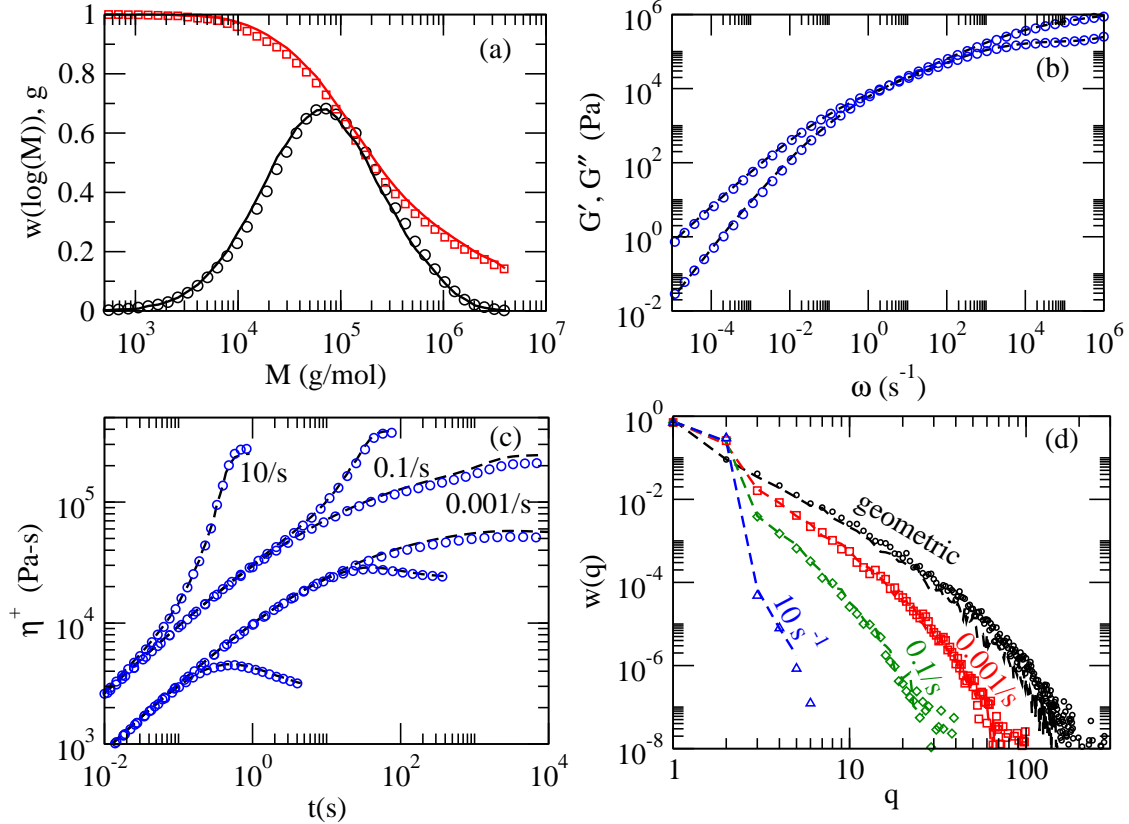
18

FIG. 9. Predictions for two different set of parameters for modelling LDPE2: (a) Distribution of molar mass and g-factor. Results from set1 are shown as symbols and from set2 are shown as lines. (b) Frequency dependence of the viscous and the elastic moduli for set1 (symbols) and set2 (dashed line) are virtually indistinguishable. (c) Start-up stress growth coefficients behave similarly for set1 (symbols) and set2 (dashed lines) in both extension (upper curves) and shear (lower curves) at the indicated flow rates. (d) Priority distributions for set1 (symbols) and set2 (dashed lines) behave similarly at the different flow rates.

in relaxation times of nearby side branches. As noted above, the scheme is expected to break down for regular comb-like molecules and similar well defined structures in which all side arms have similar lengths. Correction of this requires a more detailed consideration of stretch dynamics in such regular molecules. Such work might also lead to improvements to our proposed scheme, and in turn to improvements in predictions for industrial resins, for example by increasing priority predictions at low flow rates.

An alternative avenue for further investigation concerns the effect of dynamic dilution upon branch-point withdrawal processes and flow-rate dependent priority. Whilst the linear rheology calculation explicitly considers different tube diameters operating at different timescales via the dynamic dilution hypothesis, these considerations are not so explicit in our priority calculation as presented above. In fact, our scheme corresponds to the maximum stretch (priority) being defined in a "flow-tube" whose diameter corresponds to the dilution at the flow time τ_{F}, the inverse of flow-rate. The reason is that constraint release modes, corresponding to structure on lengthscales smaller than this "flow-tube", relax much faster than the flow time, and so are not stretched; only modes corresponding to structure on

scales larger than the "flow-tube" are stretched. However, recent investigations into bimodal blends (Auhl *et al.*, 2009; Read *et al.*, 2012) indicate that stretch relaxation dynamics in the presence of constraint release can give rise to complicated and non-intuitive dynamics. The question arises as to whether branch-point withdrawal, leading to maximum stretch, should be considered within the flow tube, or perhaps within some smaller tube. Considering a pom-pom like model, Wagner and Rolón-Garrido (2008) assumed branch-point withdrawal should occur in the undiluted tube, giving rise to a larger effective maximum stretch in the diluted tube, and so larger stresses. It is possible that similar physics might be another source of our underprediction of stress at low flow rates. Detailed investigation into this would require a consideration of stretch dynamics in the presence of a broad range of constraint release rates, in particular focusing on force balance and dynamics in the vicinity of branchpoints.

Finally, we note that recent experiments on branched polyethylene resins have indicated that there may be stress overshoots prior to the steady state in extensional flow (Wagner and Rolón-Garrido, 2008; Alvarez *et al.*, 2013; Hoyle *et al.*, 2013), though others dispute these findings (Münstedt and Starý, 2013). To date, a detailed molecular explanation of the stress overshoots appears to be lacking (for example, the model in Hoyle *et al.* (2013) is phenomenological). In this work our focus has been on developing non-linear rheology predictions based on molecular structure. We have chosen to use the established pom-pom model in our calculations, since this has a molecular basis for each of its parameters. As a result, this present work does not address directly the existence of stress overshoots.

The scheme detailed here is computationally intensive. Thus, we do not envisage the current approach to be used to predict flow properties in a complex flow geometry. Instead, the generated pom-pom modes can be coarse-grained to a more manageable numbers that predicts the same flow property as the original modes but loses the connection to the molecular architecture. Some work along this line has been done for describing large amplitude oscillatory shear experiments (Hoyle, 2010). These coarse-grained pom-pom modes in turn can be used to predict the flow properties in more complex geometries (Hassell *et al.*, 2008).

ACKNOWLEDGEMENTS

REFERENCES

Alvarez, N. J., Marín, J. M. R., Huang, Q., Michelsen, M. L., and Hassager, O., "Creep measurements confirm steady flow after stress maximum in extension of branched polymer melts," Phys. Rev. Lett. **110**, 168301 (2013).

Auhl, D., Chambon, P., McLeish, T. C. B., and Read, D. J., "Elongational flow of blends of long and short polymers: Effective stretch relaxation time," Phys. Rev. Lett. **103**, 136001 (2009).

Bick, D. K. and McLeish, T. C. B., "Topological contributions to nonlinear elasticity in branched polymers," Phys. Rev. Lett. **76**, 2587–2590 (1996).

Bisko, G., McLeish, T. C. B., Harlen, O. G., and Larson, R. G., "Theoretical molecular rheology of branched polymers in simple and complex flows: The pom-pom model," Phys. Rev. Lett. **79**, 2352–2355 (1997).

Blackwell, R. J., McLeish, T. C. B., and Harlen, O. G., "Molecular drag-strain coupling in branched polymer melts," J. Rheol. **44**, 121–136 (2000).

Chambon, P., Fernyhough, C. M., Im, K., Chang, T., Das, C., Embery, J., McLeish, T. C. B., and Read, Daniel, J., "Synthesis, temperature gradient interaction chromatography, and rheology of entangled styrene comb polymers," Macromolecules **41**, 5869–5875 (2008).

Chen, X., Stadler, F. J., Münstedt, H., and Larson, R. G., "Method for obtaining tube model parameters for commercial ethene/α-olefin copolymers," J. Rheol. **54**, 393–406 (2010).

Colby, R. H. and Rubinstein, M., "Two-parameter scaling for polymers in θ solvents," Macromolecules **23**, 2753–757 (1990).

Das, C., Inkson, N. J., Read, D. J., Kelmanson, M. A., and McLeish, T. C. B., "Computational linear rheology of general branch-on-branch polymers," J. Rheol. **50**, 207–235 (2006a).

Das, C., Read, D. J., Kelmanson, M. A., and McLeish, T. C. B., "Dynamic scaling in entangled mean-field gelation polymers," Phys. Rev. E **74**, 011404 (2006b).

Das, C. *et al..*, "bob2.5," http://sourceforge.net/projects/bob-rheology (2012).

Doi, M. and Edwards, S. F., *The theory of polymer dynamics* (Clarendon Press, Oxford, 1986).

de Gennes, P. G., "Reptation of a polymer chain in the presence of fixed obstacles," J. Chem. Phys. **55**, 572–579 (1971).

Hassell, D. G., Auhl, D., McLeish, T. C. B., and Mackley, Malcolm, R., "The effect of viscoelasticity on stress fields within polyethylene melt flow for a cross-slot and contraction–expansion slit geometry," Rheo. Acta **47**, 821–834 (2008).

Hoyle, D. M., *Constitutive modelling of branched polymer melts in non-linear response*, Ph.D. thesis, University of Leeds (2010).

Hoyle, D. M., Huang, Q., Auhl, D., Hassell, D., Rasmussen, H. K., Skov, A. L., Harlen, O. G., Hassager, O., and McLeish, T. C. B., "Transient overshoot extensional rheology of long chain branched polyethylenes: experimental and numerical comparisons between filament stretching and cross-slot flow," J. Rheol. **57**, 293–313 (2013).

Hutchings, L. R., Kimani, S. M., Hoyle, D. M., Read, D. J., Das, C., McLeish, T. C. B., Chang, T., Lee, H., and Auhl, D., "In silico molecular design, synthesis, characterization, and rheology of dendritically branched polymers: closing the design loop," ACS Macro Letters **1**, 404–408 (2012).

Inkson, N. J., McLeish, T. C. B., Harlen, O. G., and Groves, D. J., "Predicting low density polyethylene melt rheology in elongational and shear flows with "pom-pom" constitutive equations," J. Rheol. **43**, 873–896 (1999).

Klein, J., "Evidence for reptation in an entangled polymer," Nature **271**, 143–145 (1978).

Larson, R. G., "Combinatorial rheology of branched polymer melts," Macromolecules **34**, 4556–4571 (2001).

Lee, K., Mackley, M. R., McLeish, T. C. B., Nicholson, T. M., and Harlen, O. G., "Experimental observation and numerical simulation of transient "stress fangs" within flowing molten polyethylene," J. Rheol. **45**, 1261–1277 (2001).

McLeish, T. C. B., "Hierarchical relaxation in tube models of branched polymers," Europhys. Lett. **6**, 511–516 (1988).

McLeish, T. C. B. and Larson, R. G., "Molecular constitutive equations for a class of branched polymers: The pom-pom polymer," J. Rheol. **42**, 81–110 (1998).

Milner, S. T. and McLeish, T. C. B., "Parameter-free theory for stress relaxation in star polymer melts," Macromolecules **30**, 2159–2166 (1997).

Münstedt, H. and Starý,, "Steady states in extensional flow of strain hardening polymer melts and the uncertainties of their determination," J. Rheol. **57**, 1065–1077 (2013).

Park, S. J., Shanbhag, S., and Larson, R. G., "A hierarchical algorithm for predicting the linear viscoelastic properties of polymer melts with long-chain branching," Rheol. Acta **44**, 319–330 (2005).

Read, D. J., Auhl, D., Das, C., den Doelder, J., Kapnistos, M., Vittorias, I., and McLeish, T. C. B., "Linking models of polymerization and dynamics to predict branched polymer structure and flow," Science **333**, 1871–1874 (2011).

Read, D. J., Jagannathan, K., Sukumaran, S. K., and Auhl, D., "A full-chain constitutive model for bidisperse blends of linear polymers," J. Rheol. **56**, 823–873 (2012).

Read, D. J. and McLeish, T. C. B., "Molecular rheology and statistics of long chain branched metallocene-catalyzed polyolefins," Macromolecules **34**, 1928–1945 (2001).

Rubinstein, M., Zurek, S., McLeish, T. C. B., and Ball, R. C., "Relaxation of entangled polymers at the classical gel point," J. Physique **51**, 757–775 (1990).

van Ruymbeke, E., Bailly, C., Keunings, R., and Vlassopoulos, D., "A general methodology to predict the linear rheology of branched polymers," Macromolecules **39**, 6248–6259 (2006).

Tobita, H., "Simultaneous long-chain branching and random scisson: I. monte carlo simulation," J. Polymer Sc. B. **39**, 391–403 (2001).

Vivoy, J. L., Rubinstein, M., and Colby, R. H., "Constraint release in polymer melts: Tube reorganization versus tube dilation," Macromolecules **24**, 3587–3596 (1991).

Wagner, Manfred, H. and Rolón-Garrido, V. H., "Verification of branch point withdrawal in elongational flow of pom-pom polystyrene melt," J. Rheol. **52**, 1049–1068 (2008).

Wang, Z., Chen, X., and Larson, R. G., "Comparing tube models for predicting the linear rheology of branched polymer melts," J. Rheol. **54**, 223–260 (2010).

Wood-Adams, P. M., Dealy, J. M., deGroot, W. A., and Redwine, D. O., "Effect of molecular structure on the linear viscoelastic behavior of polyethylene," Macromolecules **33**, 7489–7499 (2000).